Applied Water Science (2020) 10:133
https://doi.org/10.1007/s13201-020-01216-0

ORIGINAL ARTICLE

Evaluation of diffuse fraction and diffusion coefficient using statistical analysis

Hicham Salhi[1] · **Lazhar Belkhiri**[1] · **Ammar Tiri**[1]

Received: 10 January 2020 / Accepted: 28 April 2020 / Published online: 12 May 2020

Abstract

In this study, eighty models are proposed in order to estimate the diffuse fraction and diffuse coefficient. For the proposed models, sunshine ratio and clearness index are considered as predictors. Monthly average global and diffuse solar radiation together with sunshine duration data of Tamanrasset station form 1995 to 2017 were analyzed. The different proposed models are compared and statistically analyzed to assess the performance of the best fitted model. Nine statistical indicators and Global Performance Indicator are computed to evaluate different proposed models. It is concluded that the cubic model with sunshine ratio and clearness index is selected as the best accurate model to estimate diffuse solar radiation on a horizontal surface in the study area.

Keywords Statistical analysis · Diffuse fraction · Diffusion coefficient · Sunshine ratio · Clearness index · Tamanrasset station

List of symbols

H_d	Diffuse solar radiation on a horizontal surface (MJ/m^2 day)
H	Global solar radiation on a horizontal surface (MJ/m^2 day)
H_0	Extraterrestrial radiation
k_d	Diffuse fraction (or cloudiness index)
K_D	Diffusion coefficient
K_t	Clearness index
S_t	Sunshine ratio
S_o	Maximum possible sunshine duration (h)
S	Sunshine duration (h)

Introduction

Solar energy is a renewable energy resource in nature, and it plays a major factor in between other alternative energy source. For any study of solar energy, the information of solar radiation at a given geographical location is very important (Bakirci 2009, 2015). There are many important radiation parameters such as global, diffuse and direct radiation used in solar energy techniques (Hussain et al. 1999). Solar energy in Algeria is available in abundant amounts across the year; the average duration of sunshine value is 3000 h/year. Also, the average energy is 1700 KW h/m^2/year in the North and 2650 KW h/m^2/year in the South (BoudgheneStambouli 2011; Bouchouicha et al. 2015). There are many studies carried out in the world for estimating diffuse solar radiation using the available data which include hours of solar radiation (Sabbagh et al. 1977; Iqbal 1979; Erbs et al. 1982; De Miguel et al. 2001; Paliatsos et al. 2003; Li et al. 2012).

The recent studies have used empirical models based on mathematical function to estimate the diffuse radiation using clearness index and sunshine ratio, thus playing an essential role in the absence of required technological installations. Many authors have used linear or nonlinear regression models and polynomial models to correlate diffusion coefficient or diffuse fraction with sunshine ratio and/or clearness index (Orgill and Hollands 1977; Spencer

✉ Hicham Salhi
salhiheat@gmail.com

Lazhar Belkhiri
belkhiri_laz@yahoo.fr; belkhiri.la@gmail.com

Ammar Tiri
Tiri_ammar@yahoo.fr

[1] Laboratory of Applied Research in Hydraulics, University of Mustapha Ben Boulaid-Batna 2, Batna, Algeria

1982; Reindl et al. 1990; Lam and Li 1996; Hua et al. 2002; Soares et al. 2004). Kuo et al. (2014) studied the data for global and diffuse radiation in Tainan, Taiwan, for two years; the proposed models are compared with the fourteen models available in the literature; it is concluded that the proposed piece-wise linear models perform well in predicting the diffuse fraction. Liu et al. (2017) developed four models using global solar radiation and sunshine duration data in China; the analysis of statistical indexes demonstrated that cubic models presented the best performance in radiation zone. For Algeria, Mecibah et al. (2014) proposed quadric and cubic models based on the sunshine-based models. Also, Bailek et al. (2017) reviewed and compared thirty-five proposed correlations to measured irradiation of Algerian Big South (Adrar region); it is concluded that the second-order polynomial model of diffuse fraction is able to estimate the monthly average daily diffuse irradiation on a horizontal surface.

The main objective of this study is to develop and compare different proposed empirical models for estimation of horizontal monthly mean diffuse solar radiation based on clearness index and sunshine ratio.

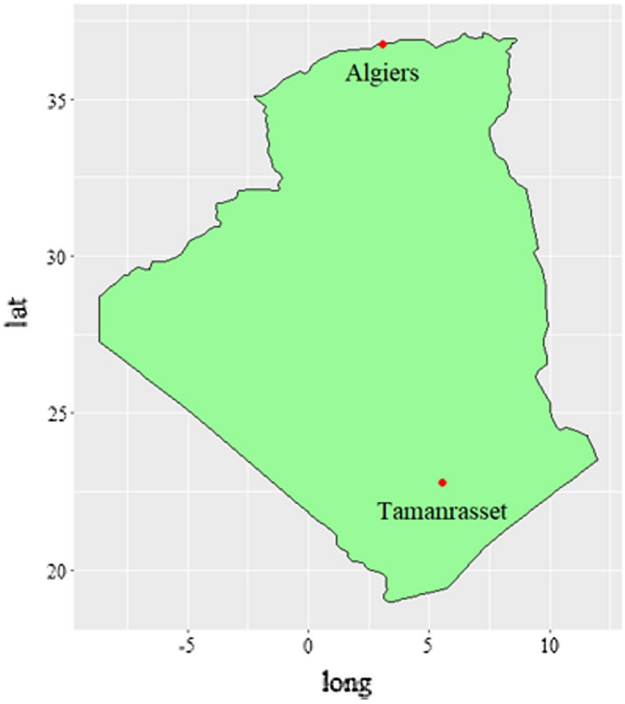

Fig. 1 Location of Tamanrasset station

Methodology

Solar radiation data

Data of horizontal global solar radiation, diffuse solar radiation and sunshine period of Tamanrasset station were taken from National Meteorological Office of Algeria from 1995 to 2017. The geographical information of the station is given in Table 1. Tamanrasset is located in the south-eastern region of Algeria (Fig. 1). Tamanrasset has a hot desert climate (Köppen climate classification BWh), with very hot summers and mild winters. There is very little rain throughout the year, although occasional rain does fall in late summer from the northern extension of the Intertropical Convergence Zone.

Table 1 Geographic and data records period of Tamanrasset

Latitude (°N)	22.78
Longitude (°E)	5.51
Elevation (m)	1378
Data series period	1995–2017
Mean GH (MJ/m^2 day)	7.26
Mean S (h)	9.20
Mean $T°$ (°C)	22.71
Mean RH (%)	28.6

Proposed of models

In the current study, the regression analysis is used for the proposed models, where the predictand is the diffuse fraction (k_d) or diffuse coefficient (K_D) and the predictors are sunshine ratio (S_t) and clearness index (K_t). Thus, three types of forty models can be defined for e diffuse fraction and diffusion coefficient. The three respective types can be written as:

$$\left(k_d = \frac{H_d}{H}, K_D = \frac{H_d}{H_0}\right) \approx f(S_t) \quad (1)$$

$$\left(k_d = \frac{H_d}{H}, K_D = \frac{H_d}{H_0}\right) \approx f(K_t) \quad (2)$$

$$\left(k_d = \frac{H_d}{H}, K_D = \frac{H_d}{H_0}\right) \approx f(S_t, K_t) \quad (3)$$

where H_0, H, and H_d are the monthly mean daily extraterrestrial solar radiation, global solar radiation and diffuse solar radiation on a horizontal surface, respectively. Mathematically, sunshine ratio and clearness index are defined as

$$K_t = \frac{H}{H_0} \quad (4)$$

$$S_t = \frac{S}{S_0} \tag{5}$$

where S and S_o are the sunshine duration and maximum possible sunshine durations, respectively.

The monthly average daily extraterrestrial solar radiation on a horizontal surface is calculated from the following equation Klein (1977):

$$H_0 = \frac{24}{\pi} H_{sc}\left(1 + 0.033\cos\left(\frac{360}{365}n\right)\right) \left(\cos\varphi\cos\delta\sin\omega_s + \frac{\pi}{180}\omega_s\sin\varphi\sin\delta\right) \tag{6}$$

where H_{sc} is the solar constant, n is the Julian day of the year, φ is the location latitude, and δ is declination angle, ω_s is the sunset hour angle. δ and ω_s are mathematically defined as:

$$\delta = 23.45\sin\left[360\frac{(n+284)}{365}\right] \tag{7}$$

$$\omega_s = \cos^{-1}\left[-\tan\varphi\tan\delta\right] \tag{8}$$

The maximum possible sunshine duration (S_0) is calculated as:

$$S_0\frac{2}{15}\omega_s \tag{9}$$

The forty proposed models for each diffuse fraction and diffusion coefficient are presented in Table 2.

Statistical evaluation

In this study, nine statistical indicators were used to evaluate different proposed models such as mean bias error (MBE), mean absolute error (MAE), mean absolute relative error (MARE), mean absolute percentage error (MAPE), root mean squared error (RMSE), root mean squared relative error (RMSRE), relative root mean squared error (RRMSE), correlation coefficient (R^2) and t-statistics (t-stat). Mathematical expressions for these indicators are defined as:

$$\text{MBE} = \frac{1}{n}\sum_{i=1}^{n}\left(H_{i,o} - H_{i,m}\right) \tag{10}$$

$$\text{MAE} = \frac{1}{n}\sum_{i=1}^{n}\left|H_{i,m} - H_{i,o}\right| \tag{11}$$

$$\text{MARE} = \frac{1}{n}\sum_{i=1}^{n}\left|\frac{H_{i,m} - H_{i,o}}{H_{i,m}}\right| \tag{12}$$

$$\text{MAPE} = \frac{1}{n}\sum_{i=1}^{n}\left|\frac{H_{i,m} - H_{i,o}}{H_{i,o}}\right| * 100 \tag{13}$$

$$\text{RMSE} = \sqrt{\frac{1}{n}\sum_{i=1}^{n}\left(H_{i,m} - H_{i,o}\right)^2} \tag{14}$$

$$\text{RMSRE} = \sqrt{\frac{1}{n}\sum_{i=1}^{n}\left(\frac{H_{i,m} - H_{i,o}}{H_{i,m}}\right)^2} \tag{15}$$

$$\text{RRMSE} = \sqrt{\frac{\frac{1}{n}\sum_{i=1}^{n}\left(H_{i,m} - H_{i,o}\right)^2}{\frac{1}{n}\sum_{i=1}^{n}H_{i,m}}} * 100 \tag{16}$$

$$R^2 = 1 - \frac{\sum_{i=1}^{n}\left(H_{i,m} - H_{i,o}\right)^2}{\sum_{i=1}^{n}\left(H_{i,m} - \overline{H_m}\right)} \tag{17}$$

$$t\text{ - stat} = \sqrt{\frac{(n-1)\text{MBE}^2}{\text{RMSE}^2 - \text{MBE}^2}} \tag{18}$$

where n is the number of the solar irradiation data, $H_{i,m}$ is the ith estimated values, $H_{i,o}$ is the ith observed values and $\overline{H_m}$ is the estimated mean value.

Results and discussion

The statistical descriptive of diffuse solar radiation includes minimum, maximum, mean, standard deviation and coefficient of variance is shown in Table 3. The mean value of global and diffuse solar radiation is 2320 and 704.2 MJ/m^2 day with a standard deviation of 394.4 and 282.35 MJ/m^2 day, respectively. The coefficient of variance of H and H_d is 17 and 40%, respectively. The diffuse fraction and diffusion coefficient values ranged from 0.105 to 0.577 and 0.030 to 0.121 with a mean of 0.298 and 0.074, respectively. High values of k_d and K_D are observed in the months of April, May, June, July, August and September (Fig. 2).

The values of sunshine ratio and clearness index varied from 0.205 to 0.298 and 7.105 to 16.401 with a mean of 0.251 and 12.826, respectively, where high values for both predictors (S_t and K_t) are observed between the months of January to December (Fig. 2). From the Fig. 3, it was observed that there is a significant negative correlation between k_d–S_t (−0.859), k_d–K_t (−0.722), K_D–S_t (−0.825), and K_D–K_t (−0.577).

The statistical indicators of the different models are given in Table 4. For higher modeling accuracy MBE,

Table 2 (a) Various forms of correlations for diffuse fraction and (b) various forms of correlations for diffusion coefficient

	Models	Forms of the models
(a)		
$k_d \approx f(S_t)$	M1	$K_d = 0.8671 - 0.044S_t$
	M2	$K_d = 0.6498 - 0.0084S_t - 0.0014S_t^2$
	M3	$K_d = 0.27947 + 0.0884S_t - 0.0096S_t^2 + 0.00022S_t^3$
	M4	$K_d = 1.6363 - 0.527\log(S_t)$
	M5	$K_d = 0.338 - 3.165e-08(S_t)$
$k_d \approx f(K_t)$	M6	$K_d = 1.244 - 3.7667K_t$
	M7	$K_d = 2.7023 - 15.5047K_t + 23.4966K_t^2$
	M8	$K_d = -2.149 + 43.268K_t - 212.6799K_t^2 + 314.852K_t^3$
	M9	$K_d = -1.0036 - 0.9405\log(K_t)$
	M10	$K_d = 4.0634 - 2.9283\exp(K_t)$
$k_d \approx f(S_t, K_t)$	M11	$K_d = 1.0773 - 1.284K_t - 0.0356S_t$
	M12	$K_d = 0.862 - 1.2834 - 0.0014S_t^2$
	M13	$K_d = 0.8038 - 1.3563K_t - 0.000073S_t^3$
	M14	$K_d = 1.5634 - 5.21K_t + 7.8084K_t^2 - 0.03525S_t$
	M15	$K_d = 1.6769 - 7.8387K_t + 13.0676K_t^2 - 0.0014S_t^2$
	M16	$K_d = 1.9146 - 10.289K_t + 17.8432K_t^2 - 7.3165e-05S_t^3$
	M17	$K_d = 1.732 - 8.9753K_t + 15.2995K_t^2 + 0.0143S_t - 0.0019S_t^2$
	M18	$K_d = 1.3754 - 9.2057K_t + 15.7663K_t^2 + 0.1147S_t - 0.0105S_t^2 + 0.00023S_t^3$
	M19	$K_d = 1.7641 - 8.7455K_t + 14.8467K_t^2 - 8.88e-04S_t^2 - 2.769e-05S_t^3$
	M20	$K_d = 6.8129 - 68.8458K_t + 263.825K_t^2 - 341.546K_t^3 - 0.0356S_t$
	M21	$K_d = 10.898 - 120.453K_t + 462.173K_t^2 - 594.048K_t^3 + 241.606S_t - 2.412e-03S_t^2$
	M22	$K_d = 10.548 - 114.886K_t + 440.302K_t^2 - 565.56K_t^3 - 0.00561S_t - 6.385e-05S_t^3$
	M23	$K_d = 12.261 - 145.598K_t + 562.111K_t^2 - 725.735K_t^3 + 0.214S_t - 0.0184S_t^2 + 4.42e-04S_t^3$
	M24	$K_d = 10.465 - 114.178K_t + 437.801K_t^2 - 562.654K_t^3 - 5.79e-04S_t^2 - 4.54e-05S_t^3$
	M25	$K_d = 9.3589 - 100.998K_t + 387.842K_t^2 - 499.905K_t^3 - 0.00145S_t^2$
	M26	$K_d = 11.138 - 122.15K_t + 467.77K_t^2 - 600.016K_t^3 - 7.517e-05S_t^3$
	M27	$K_d = 1.3911 - 3.1948K_t + 10.027K_t^3 - 0.0352S_t$
	M28	$K_d = 1.398 - 5.021K_t + 19.616K_t^3 + 0.0135S_t - 0.0019S_t^2$
	M29	$K_d = 1.48 - 4.951K_t + 19.247K_t^3 - 0.0101S_t - 5.276e-05S_t^3$
	M30	$K_d = 1.041 - 5.116K_t + 20.136K_t^3 + 0.11S_t - 0.0102S_t^2 + 0.00022S_t^3$
	M31	$K_d = 1.437 - 4.912K_{t+} + 19.057K_t^3 - 9.203e-04S_t^2 - 2.601e-05S_t^3$
	M32	$K_d = 1.391 - 4.4841K_t + 16.87K_t^3 - 0.0014S_t^2$
	M33	$K_d = 1.528 - 5.728K_t + 23.129K_t^3 - 7.31e-05S_t^3$
	M34	$K_d = 0.862 - 0.347 - 0.1\log(S_t)$
	M35	$K_d = 3.084 - 2.148\exp(K_t) - 1.87e-08\exp(S_t)$
	M37	$K_d = -0.2163 + 25.814\left(\frac{K_t}{S_t}\right)$
	M38	$K_d = -0.8485 + 86.043\left(\frac{K_t}{S_t}\right) - 1409.06\left(\frac{K_t}{S_t}\right)^2$
	M39	$K_d = 0.061 + 587.079\left(\frac{K_t}{S_t}\right)^2$
	M40	$K_d = 0.155 + 1.714e+04\left(\frac{K_t}{S_t}\right)^3$

Table 2 (continued)

	Models	Forms of the models
(b)		
$K_D \approx f(S_t)$	M41	$K_D = 0.1869 - 0.0088S_t$
	M42	$K_D = 0.0913 + 0.0069S_t - 0.0006S_t^2$
	M43	$K_D = 0.0178 - 0.0261S_t - 2.27e-03S_t^2 + 4.522993e-05S_t^3$
	M44	$K_D = 0.337 - 0.1039\log(S_t)$
	M45	$K_D = 0.082 - 6.736e-09\exp(S_t)$
$K_D \approx f(K_t)$	M46	$K_D = 0.2304 - 0.624K_t$
	M47	$K_D = 0.3742 - 1.781K_t + 2.3171K_t^2$
	M48	$K_D = -1.4 + 19.719K_t - 84.085K_t^2 + 115.184K_t^3$
	M49	$K_D = -0.141 - 0.155\log(K_t)$
	M50	$K_D = 0.698 - 0.485\exp(K_t)$
$K_D \approx f(S_t, K_t)$	M51	$K_D = 0.189 - 0.015K_t - 0.0087S_t$
	M52	$K_D = 0.135 - 0.0064K_t - 0.00035S_t^2$
	M53	$K_D = 0.119 - 0.0174K_t - 1.857e-05S_t^3$
	M54	$K_D = 0.089 + 0.7918K_t - 1.605K_t^2 - 0.0088S_t$
	M55	$K_D = 0.1160 + 0.1486K_t - 0.3093K_t^2 - 0.00035S_t^2$
	M56	$K_D = 0.1745 - 0.46K_t + 0.884K_t^2 - 1.854e-05S_t^3$
	M57	$K_D = 0.1464 - 0.48K_t + 0.925K_t^2 + 0.0079S_t - 0.0006S_t^2$
	M58	$K_D = 0.074 - 0.526K_t + 1.019K_t^2 + 0.028S_t - 2.39e-03S_t^2 4.77e-05S_t^3$
	M59	$K_D = 0.17 - 0.413K_t + 0.793K_t^2 - 2.69e-05S_t^2 - 1.71e-05S_t^3$
	M60	$K_D = 0.828 - 8.168K_t + 34.445K_t^2 - 48.093K_t^3 - 0.0088S_t$
	M61	$K_D = 2.121 - 24.497K_t + 97.204K_t^2 - 127.98K_t^3 + 1.005e-02S_t - 7.63e-04S_t^2$
	M62	$K_D = 2.024 - 22.905K_t + 90.932K_t^2 - 119.79K_t^3 + 7.47e-04S_t - 2.04e-05S_t^3$
	M63	$K_D = 2.404 - 29.725K_t + 117.98K_t^2 - 155.36K_t^3 + 4.96e-02S_t + 0.0901S_t^2 - 4.105e-03S_t^3$
	M64	$K_D = 1.989 - 22.456K_t + 89.222K_t^2 - 117.636K_t^3 + 3.77e-05S_t^2 - 2.086e-05S_t^3$
	M65	$K_D = 1.48 - 16.398K_t + 66.26K_t^2 - 88.795K_t^3 - 3.636e-04S_t^2$
	M66	$K_D = 1.945 - 21.937K_t 87.272K_t^2 - 115.205K_t^3 - 1.89e-05S_t^3$
	M67	$K_D = 0.1208 + 0.4025K_t - 2.192K_t^3 - 0.0088S_t$
	M68	$K_D = 0.1233 - 0.2202K_t + 1.0782K_t^3 + 0.0078S_t - 0.00066S_t^2$
	M69	$K_D = 0.1516 - 0.2017K_t 0.979K_t^3 - 1.99e-04S_t - 1.814e-05S_t^3$
	M70	$K_D = 0.049 - 0.2398K +_t 1.185K_t^3 + 0.0278S_t - 2.36e-03S_t^2 + 4.7e-05S_t^3$
	M71	$K_D = 0.1494 - 0.188K_t + 0.9141K_t^3 - 3.18e-05S_t^2 - 1.691711e-05S_t^3$
	M72	$K_D = 0.1193 + 0.0899K_t - 0.5084K_t^3 - 0.00035S_t^2$
	D73	$K_D = 0.1525 - 0.2168K_t + 1.0548K_t^3 - 1.854e-05S_t^3$
	M74	$K_D = 0.3133 - 0.0108\log(K_t) - 0.1003\log(S_t)$
	M75	$K_D = 0.4326 - 0.274\exp(K_t) - 5.091e-09\exp(S_t)$
	M76	$K_D = -0.0382 + 5.6124\left(\frac{K_t}{S_t}\right)$
	M77	$K_D = -0.2473 + 25.538\left(\frac{K_t}{S_t}\right) - 466.17\left(\frac{K_t}{S_t}\right)^2$
	M78	$K_D = 6.058e-02 - 17.445\left(\frac{K_t}{S_t}\right) + 1501.46\left(\frac{K_t}{S_t}\right)^2 - 29502.33\left(\frac{K_t}{S_t}\right)^3$
`	M79	$K_D = 0.0227 + 126.302\left(\frac{K_t}{S_t}\right)^2$
	M80	$K_D = 0.0433 + 3647.46\left(\frac{K_t}{S_t}\right)^3$

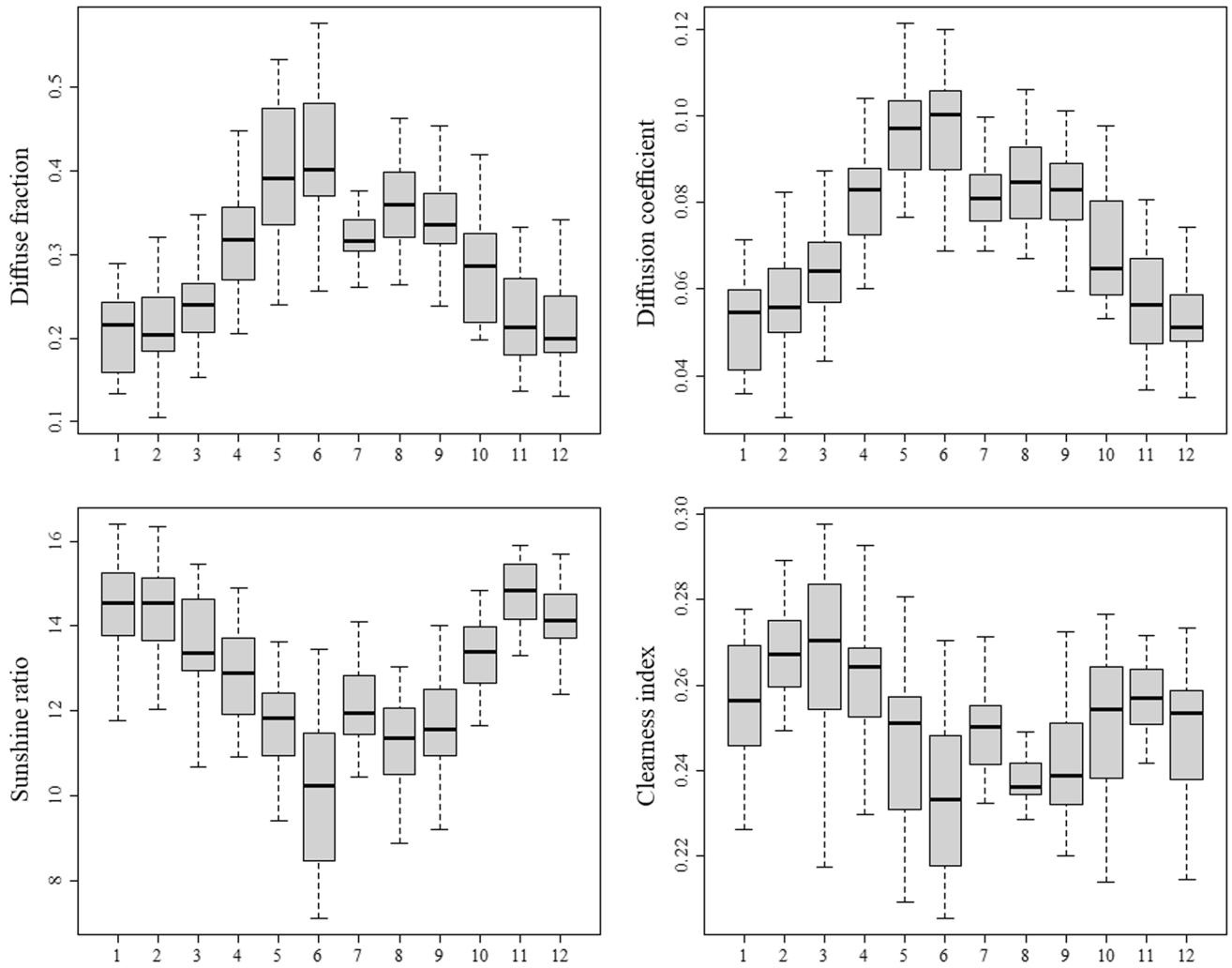

Fig. 2 Box plot of diffuse fraction (top left), diffusion coefficient (top right), sunshine ratio (bottom left) and clearness index (bottom right)

MAE, MARE, MAPE, RMSE, RMSRE, RRMSE and *t*-stat indicators should be closer to zero, but correlation coefficient (R^2) should approach to 1 as closely as possible. From the statistical indicators, it can be seen that the estimated values of k_d and K_D are in good agreement with the measured values for the most models. The values of MBE are ranged from $-1.68\ e^{-17}$ to $9.84\ e^{-18}$ and $-1.81\ e^{-18}$ to $1.06\ e^{-18}$ for k_d and K_D, respectively. We observed that the MBE values for the different models are very small which means that the proposed models slightly over predict the estimated values. The values of t-stats obtained for the all proposed models are significantly lower than the critical value. In terms of MBE and *t*-stats, the models M40 for k_d and M65 for K_D show the lowest errors. However, in terms of MAE, MARE, MAPE, RMSE, RMSRE, and RRMSE, the cubic model for both k_d and K_D (M23 for k_d and M63 for K_D) shows excellent accuracy since the MAE, MARE, MAPE, RMSE, RMSRE, and RRMSE values are the lowest. The correlation coefficient (R^2) is observed to be the highest for M23 (k_d) and M63 (K_D) among all the models proposed, which means that the estimated and observed data from the cubic equations shows a maximum closeness.

The results of the statistical indicators show that the estimated diffuse fraction and diffuse coefficient values from the different proposed models are close to each other. Since not all the statistical indicators are in favor of a model, more appropriate combined statistical indicators which can yield a comparative performance of the proposed models need to be established. In this way, we used Global Performance Indicator (GPI) that represents multiplication of all used statistical indicators (Said and Dickey 1983; Despotovic et al. 2015; Jamil and Abid 2018).

Table 3 Statistical descriptive of diffuse solar radiation

Parameters	H	H_d	k_d	K_D	K_t	S_t
Min	1441	235	0.105	0.030	0.205	7.105
Max	3084	1334	0.577	0.121	0.298	16.401
Mean	2320	704.2	0.298	0.074	0.251	12.826
SD	394.4	282.35	0.097	0.020	0.019	1.870
Coef.var	0.17	0.4	0.325	0.273	0.074	0.146

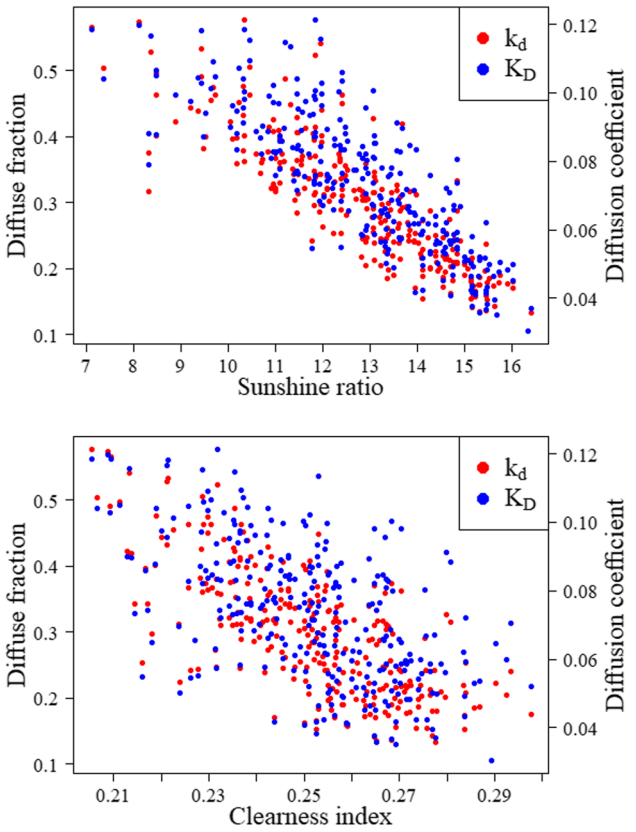

Fig. 3 Scatter plots for diffuse fraction (k_d) and diffusion coefficient (K_D) with sunshine ratio (in the top) and clearness index (in the bottom)

$$\mathrm{GPI}_i = \sum_{j=1}^{9} \alpha_j \left(y_j - y_{ij}\right) \tag{19}$$

where α_j is weight factor and equals 1 for all indicators, while correlation coefficient (R^2) is equal to -1. y_j is the median of the scaled values of indicator j, and y_{ij} is the scaled value of indicator j for model i. A higher value of GPI indicates more accurate model leading to better estimations.

The values of GPI and ranking of the model are shown in Table 5. The GPI of the proposed models ranged from -4.803 to 0.309 and -5.70 to 0.23 for k_d and K_D, respectively. The highest GPI shows the best performing model. Form the Table 5, we observed among the models, 33% and 43% of the total models attain a positive GPI value and the other models have a negative GPI. The maximum value of GPI is observed for model 23 (GPI = 0.309) for k_d models and model 63 (GPI = 0.230) for K_D models. Thus, it can be inferred that the cubic model best estimates the e diffuse fraction and diffusion coefficient for the study area (Figs. 4, 5).

Table 4 Results of statistical indicators for all proposed models

Models	MBE	MAE	MARE	MAPE	RMSE	RMSRE	RRMSE	R^2	t-stat
	k_d								
M1	5.62E−19	0.0362	0.1233	12.6151	0.0493	0.1638	9.0407	0.7385	1.89E−16
M2	2.75E−18	0.0362	0.1236	12.5850	0.0489	0.1632	8.9641	0.7429	9.32E−16
M3	2.06E−18	0.0362	0.1232	12.5533	0.0488	0.1627	8.9533	0.7435	7.00E−16
M4	−7.50E−19	0.0376	0.1284	13.2475	0.0512	0.1701	9.3866	0.7181	2.43E−16
M5	−1.70E−18	0.0567	0.2223	20.9577	0.0734	0.4064	13.4539	0.4209	3.84E−16
M6	1.20E−18	0.0541	0.1879	20.4662	0.0667	0.2347	12.2255	0.5218	2.98E−16
M7	2.32E−18	0.0530	0.1819	20.0034	0.0659	0.2260	12.0829	0.5329	5.83E−16
M8	−5.51E−18	0.0530	0.1815	19.9259	0.0658	0.2255	12.0668	0.5342	1.39E−15
M9	−1.68E−17	0.0537	0.1856	20.2942	0.0663	0.2306	12.1502	0.5277	4.20E−15
M10	−1.20E−18	0.0542	0.1886	20.5140	0.0668	0.2360	12.2491	0.5200	2.97E−16
M11	9.84E−18	0.0354	0.1206	12.3883	0.0462	0.1538	8.4745	0.7702	3.53E−15
M12	−1.23E−18	0.0355	0.1216	12.4322	0.0458	0.1534	8.3934	0.7746	4.46E−16
M13	1.78E−18	0.0362	0.1257	12.7949	0.0462	0.1575	8.4617	0.7709	6.39E−16
M14	−1.59E−19	0.0354	0.1207	12.4246	0.0461	0.1532	8.4524	0.7714	5.71E−17
M15	3.08E−18	0.0353	0.1204	12.3687	0.0454	0.1514	8.3298	0.7780	1.13E−15
M16	5.05E−18	0.0355	0.1218	12.4955	0.0455	0.1529	8.3430	0.7773	1.84E−15
M17	−1.12E−18	0.0353	0.1209	12.4055	0.0454	0.1516	8.3187	0.7786	4.11E−16
M18	−4.40E−18	0.0353	0.1205	12.3795	0.0453	0.1511	8.3063	0.7793	1.61E−15
M19	3.00E−18	0.0353	0.1208	12.4036	0.0454	0.1516	8.3221	0.7784	1.10E−15
M20	1.42E−18	0.0351	0.1198	12.3273	0.0460	0.1531	8.4259	0.7729	5.13E−16
M21	6.45E−18	0.0348	0.1195	12.2581	0.0450	0.1519	8.2431	0.7826	2.38E−15
M22	7.37E−19	0.0348	0.1198	12.2837	0.0450	0.1521	8.2558	0.7819	2.71E−16
M23	2.96E−19	0.0347	0.1184	12.1390	0.0447	0.1510	8.2026	0.7847	1.10E−16
M24	3.11E−18	0.0348	0.1195	12.2610	0.0450	0.1519	8.2528	0.7821	1.14E−15
M25	2.95E−19	0.0347	0.1187	12.1870	0.0451	0.1512	8.2727	0.7810	1.08E−16
M26	−1.34E−18	0.0349	0.1205	12.3476	0.0451	0.1530	8.2615	0.7816	4.94E−16
M27	−1.97E−18	0.0354	0.1208	12.4266	0.0461	0.1532	8.4540	0.7713	7.08E−16
M28	2.46E−18	0.0353	0.1209	12.4123	0.0454	0.1517	8.3238	0.7783	8.99E−16
M29	−7.86E−18	0.0354	0.1210	12.4188	0.0454	0.1518	8.3299	0.7780	2.87E−15
M30	−1.78E−18	0.0354	0.1206	12.3866	0.0453	0.1512	8.3122	0.7790	6.51E−16
M31	4.89E−18	0.0353	0.1209	12.4092	0.0454	0.1517	8.3270	0.7782	1.78E−15
M32	−1.62E−19	0.0353	0.1205	12.3750	0.0455	0.1515	8.3338	0.7778	5.91E−17
M33	1.15E−18	0.0356	0.1220	12.5096	0.0456	0.1530	8.3495	0.7770	4.20E−16
M34	5.97E−18	0.0365	0.1248	12.9129	0.0477	0.1587	8.7395	0.7556	2.08E−15
M35	7.60E−18	0.0472	1.7216	17.5514	0.0586	25.4900	10.7396	0.6310	2.15E−15
M36	−1.01E−18	0.0550	0.1912	20.5253	0.0730	0.2586	13.3757	0.4276	2.28E−16
M37	2.52E−18	0.0532	0.1872	19.7012	0.0717	0.2677	13.1441	0.4473	5.82E−16
M38	−2.01E−18	0.0536	0.1873	19.8362	0.0713	0.2579	13.0705	0.4534	4.68E−16
M39	1.98E−19	0.0563	0.1948	21.1221	0.0742	0.2586	13.6087	0.4075	4.42E−17
M40	1.96E−19	0.0583	0.2002	21.9386	0.0760	0.2609	13.9277	0.3794	4.28E−17
	K_D								
M41	1.06E−18	0.0088	0.1214	12.4840	0.0113	0.1552	4.1724	0.6805	1.55E−15
M42	1.22E−19	0.0086	0.1198	12.2569	0.0110	0.1510	4.0407	0.7003	1.85E−16
M43	−4.73E−19	0.0086	0.1196	12.2411	0.0109	0.1507	4.0369	0.7009	7.16E−16
M44	−5.60E−19	0.0092	0.1268	13.1286	0.0119	0.1624	4.3750	0.6487	7.83E−16
M45	4.23E−19	0.0121	0.3212	17.9279	0.0149	2.2351	5.5106	0.4426	4.70E−16
M46	2.88E−19	0.0133	0.1836	20.1637	0.0163	0.2277	6.0281	0.3330	2.92E−16
M47	−4.01E−20	0.0132	0.1822	20.0393	0.0163	0.2262	6.0168	0.3355	4.08E−17
M48	1.42E−19	0.0132	0.1816	19.9307	0.0163	0.2255	5.9992	0.3394	1.45E−16
M49	−8.45E−19	0.0132	0.1827	20.0859	0.0163	0.2268	6.0201	0.3348	8.59E−16
M50	8.89E−19	0.0133	0.1839	20.1882	0.0164	0.2279	6.0314	0.3323	9.02E−16
M51	7.51E−19	0.0088	0.1216	12.5056	0.0113	0.1551	4.1717	0.6806	1.10E−15
M52	−1.84E−19	0.0086	0.1194	12.2431	0.0110	0.1514	4.0664	0.6965	2.77E−16
M53	−2.31E−19	0.0087	0.1202	12.3079	0.0110	0.1513	4.0442	0.6998	3.49E−16
M54	4.98E−19	0.0088	0.1211	12.4348	0.0113	0.1550	4.1640	0.6817	7.32E−16

Table 4 (continued)

Models	MBE	MAE	MARE	MAPE	RMSE	RMSRE	RRMSE	R^2	t-stat
M55	9.65E−20	0.0086	0.1194	12.2337	0.0110	0.1515	4.0661	0.6965	1.45E−16
M56	−2.52E−20	0.0087	0.1201	12.3066	0.0110	0.1510	4.0417	0.7002	3.81E−17
M57	−3.03E−19	0.0087	0.1199	12.2913	0.0109	0.1508	4.0378	0.7007	4.59E−16
M58	−7.03E−19	0.0087	0.1197	12.2747	0.0109	0.1505	4.0335	0.7014	1.07E−15
M59	−1.81E−18	0.0087	0.1200	12.2963	0.0110	0.1510	4.0416	0.7002	2.73E−15
M60	1.23E−19	0.0087	0.1209	12.4151	0.0113	0.1550	4.1597	0.6824	1.80E−16
M61	−7.23E−19	0.0086	0.1187	12.1584	0.0109	0.1506	4.0085	0.7051	1.10E−15
M62	−9.15E−20	0.0086	0.1189	12.1826	0.0109	0.1509	4.0158	0.7040	1.39E−16
M63	−3.28E−19	0.0085	0.1179	12.0803	0.0108	0.1500	3.9940	0.7072	5.02E−16
M64	−7.76E−19	0.0086	0.1188	12.1755	0.0109	0.1509	4.0163	0.7039	1.18E−15
M65	0.00	0.0086	0.1184	12.1320	0.0110	0.1512	4.0512	0.6988	0.000
M66	−7.76E−19	0.0086	0.1187	12.1618	0.0109	0.1507	4.0166	0.7039	1.18E−15
M67	−3.75E−19	0.0088	0.1211	12.4329	0.0113	0.1550	4.1636	0.6818	5.51E−16
M68	−3.53E−19	0.0087	0.1199	12.2903	0.0110	0.1508	4.0383	0.7007	5.35E−16
M69	6.78E−19	0.0087	0.1200	12.3011	0.0110	0.1510	4.0421	0.7001	1.03E−15
M70	6.31E−19	0.0087	0.1197	12.2746	0.0109	0.1505	4.0342	0.7013	9.56E−16
M71	6.07E−19	0.0087	0.1200	12.2949	0.0110	0.1510	4.0420	0.7001	9.18E−16
M72	−2.06E−19	0.0086	0.1194	12.2309	0.0110	0.1515	4.0659	0.6966	3.09E−16
M73	−6.30E−19	0.0087	0.1201	12.3073	0.0110	0.1511	4.0422	0.7001	9.54E−16
M74	−2.82E−20	0.0092	0.1274	13.2006	0.0118	0.1622	4.3697	0.6495	3.95E−17
M75	−5.05E−19	0.0113	0.2173	16.8329	0.0138	0.7882	5.1027	0.5221	6.05E−16
M76	2.03E−19	0.0113	0.1575	16.6378	0.0146	0.2070	5.3764	0.4694	2.31E−16
M77	−8.06E−19	0.0104	0.1480	15.2410	0.0139	0.2115	5.1171	0.5194	9.63E−16
M78	−7.76E−19	0.0104	0.1483	15.3289	0.0138	0.2062	5.1023	0.5221	9.30E−16
M79	3.28E−19	0.0117	0.1625	17.3442	0.0150	0.2098	5.5332	0.4380	3.63E−16
M80	3.28E−19	0.0122	0.1685	18.1671	0.0155	0.2144	5.7230	0.3988	3.51E−16

Table 5 The global performance indicator (GPI) and ranking for all proposed models

Models	GPI	Rank	Models	GPI	Rank	Models	GPI	Rank	Models	GPI	Rank
	k_d										
M1	−0.245	20	M11	−1.058	28	M21	−0.504	25	M31	−0.382	22
M2	−0.462	24	M12	0.128	9	M22	0.206	5	M32	0.225	3
M3	−0.373	21	M13	−0.136	16	M23	0.309	1	M33	0.054	11
M4	−0.507	26	M14	0.157	7	M24	−0.088	15	M34	−0.796	27
M5	−4.321	37	M15	−0.150	18	M25	0.269	2	M35	−4.803	40
M6	−3.543	32	M16	−0.427	23	M26	0.217	4	M36	−4.125	36
M7	−3.480	31	M17	0.178	6	M27	0.067	10	M37	−4.052	35
M8	−3.361	29	M18	0.022	13	M28	−0.078	14	M38	−3.843	34
M9	−3.729	33	M19	−0.143	17	M29	−0.168	19	M39	−4.378	38
M10	−3.476	30	M20	0.024	12	M30	0.149	8	M40	−4.727	39
	K_D										
M41	−1.009	28	M51	−0.744	27	M61	0.109	9	M71	−0.380	21
M42	0.069	14	M52	0.110	7	M62	0.224	2	M72	0.109	8
M43	0.090	11	M53	0.113	5	M63	0.230	1	M73	0.036	17
M44	−0.634	26	M54	−0.489	24	M64	0.083	13	M74	−0.561	25
M45	−5.679	39	M55	0.063	15	M65	0.204	3	M75	−3.290	32
M46	−5.257	38	M56	0.160	4	M66	0.086	12	M76	−3.203	31
M47	−4.994	35	M57	0.113	6	M67	−0.117	18	M77	−2.334	30
M48	−5.046	37	M58	0.039	16	M68	0.102	10	M78	−2.331	29
M49	−5.031	36	M59	−0.201	20	M69	−0.446	23	M79	−3.507	33
M50	−5.703	40	M60	−0.142	19	M70	−0.387	22	M80	−4.029	34

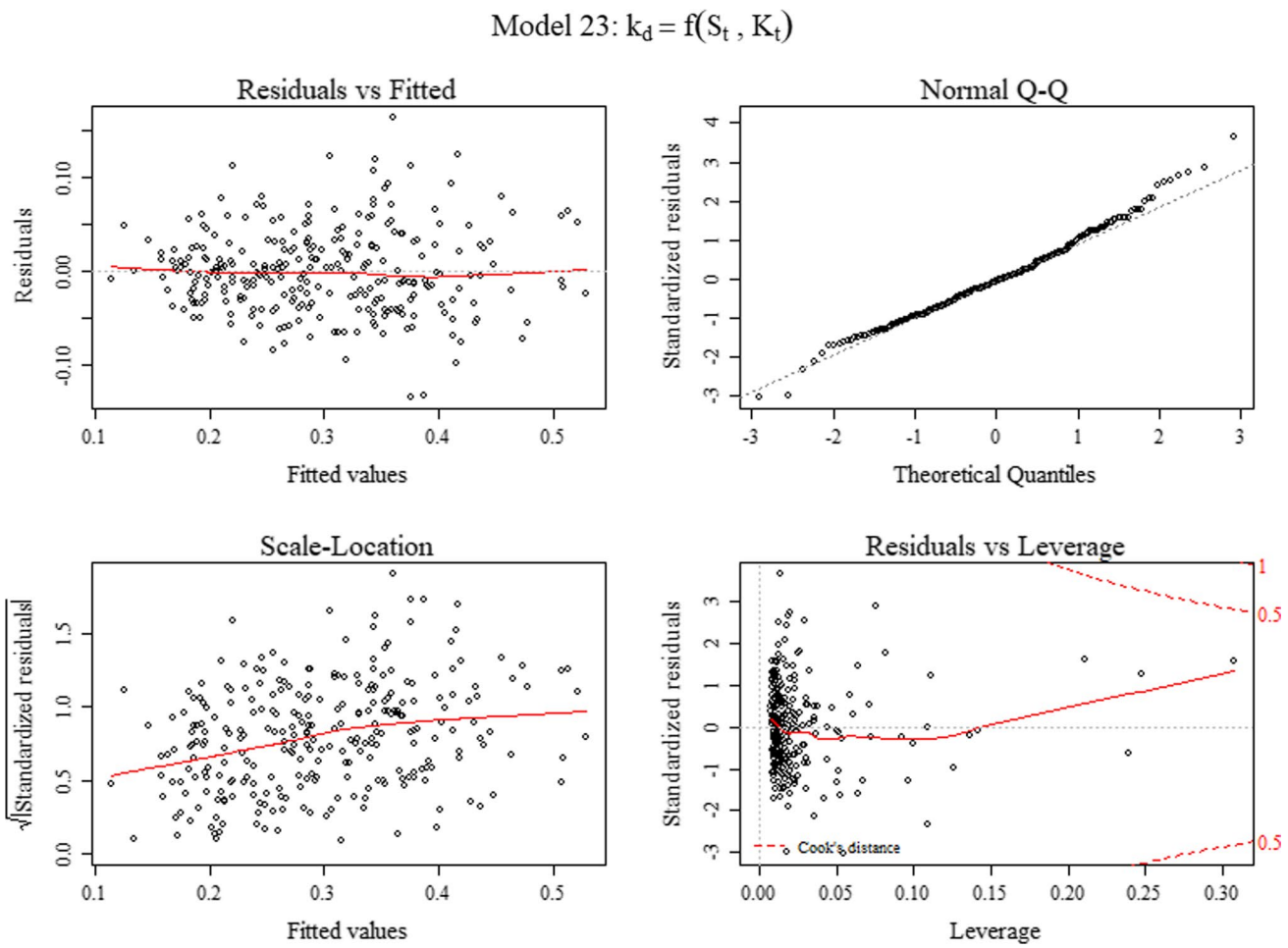

Fig. 4 Diagnostic plots of the best model of k_d (M23)

Conclusion

In this study, solar radiation data was used to evaluation the diffuse fraction and diffusion coefficient using sunshine ratio and clearness index as predictors in Tamanrasset station, Algeria. The results show that the high values of k_d and K_D are observed between the months of April to September; however, those of S_t and K_t are observed between the months of January to December. Significant negative correlation between k_d–S_t, k_d–K_t, K_D–S_t, and K_D K_t. Forty models are proposed in order to estimate the diffuse fraction and diffusion coefficient using sunshine ratio and clearness index as predictors. Based on the values of different statistical indicators and GPI, the best models for diffuse fraction and diffusion coefficient are models 23 and 63, respectively.

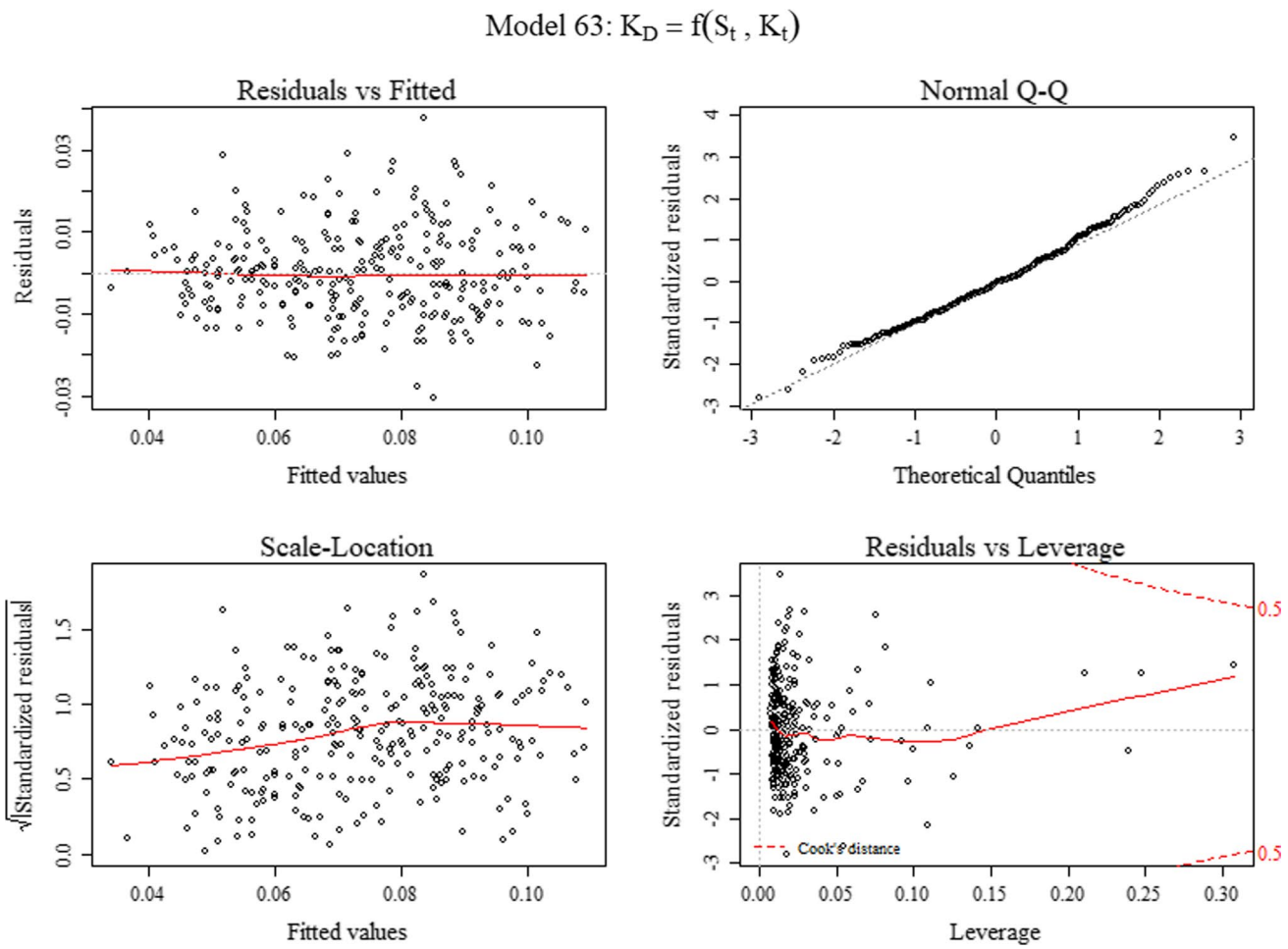

Fig. 5 Diagnostic plots of the best model of K_D (M63)

Compliance with ethical standards

Conflict of interest The authors declare that there is no conflict of interest in the publication of this article.

References

Bailek N, Bouchouicha K, Al-Mostafa Z, El-Shimy M, Aoun N, Slimani A, Al- Shehri S (2017) A new empirical model for forecasting the diffuse solar radiation over Sahara in the Algerian Big South. Renew Energy. https://doi.org/10.1016/j.renene.2017.10.081

Bakirci K (2009) Correlations for estimation of daily global solar radiation with hours of bright sunshine in Turkey. Energy 34(4):485–501

Bakirci K (2015) Models for the estimation of diffuse solar radiation for typical cities in Turkey. Energy 82:827–838

Bouchouicha K, Razagui A, Bachari NEI, Aoun N (2015) Mapping and geospatial analysis of solar resource in Algeria. Int J Energy Environ Econ 23:735

BoudgheneStambouli A (2011) Algerian renewable energy assessment: the challenge of sustainability. Energy Policy 39:4507–4519

De Miguel A, Bilbao J, Aguiar R, Kambezidis H, Negro E (2001) Diffuse solar irradiation model evaluation in the north Mediterranean belt area. Sol Energy 70(2001):143–153

Despotovic M, Nedic V, Despotovic D, Cvetanovic S (2015) Review and statistical analysis of different global solar radiation sunshine models. Renew Sustain Energy Rev 56:1869–1880

Erbs D, Klein S, Duffie J (1982) Estimation of the diffuse radiation fraction for hourly, daily and monthly-average global radiation. Sol Energy 28:293–302

Hua S, Shengyuan T, Fenxian S (2002) Models to separate daily diffuse radiation from daily total radiation for energy consumption analysis of air conditioning system. J Chongqing Univ (Nat Sci Ed) 25:73–76

Hussain M, Rahman L, Mohibur Rahman M (1999) Techniques to obtain improved predictions of global radiation from sunshine duration. Renew Energy. 18:263–275

Iqbal M (1979) A study of Canadian diffuse and total solar radiation data—I monthly average daily horizontal radiation. Sol Energy 22:81–86

Jamil B, Abid T (2018) Siddiqui. Estimation of monthly mean diffuse solar radiation over India: performance of two variable models under different climatic zones. Sustain Energy Technol Assess 25:161–180

Klein SA (1977) Calculation of monthly average insolation on tilted surfaces. Sol Energy 19:325–330

Kuo CW, Chang WC, Chang KC (2014) Modeling the hourly solar diffuse fraction in Taiwan. Renew Energy 66:56–61

Lam JC, Li DHW (1996) Correlation between global solar radiation and its direct and diffuse components. Build Environ 31:527–535

Li H, Bu X, Lian Y, Zhao L, Ma W (2012) Further investigation of empirically derived models with multiple predictors in estimating monthly average daily diffuse solar radiation over China. Renew Energy 44:469–473

Liu Y, Zhou Y, Wang D, Wang Y, Li Y, Zhu Y (2017) Classification of solar radiation zones and general models for estimating the daily global solar radiation on horizontal surfaces in China. Energy Convers Manag 154:168–179

Mecibah MS, Boukelia TE, Tahtah R, Gairaa K (2014) Introducing the best model for estimation the monthly mean daily global solar radiation on a horizontal surface (case study: Algeria). Renew Sustain Energy Rev 36:194–202

Orgill JF, Hollands KGT (1977) Correlation equation for hourly diffuse radiation on a horizontal surface. Sol Energy 19:357–359

Paliatsos A, Kambezidis H, Antoniou A (2003) Diffuse solar irradiation at a location in the Balkan Peninsula. Renew Energy 28:2147–2156

Reindl DT, Beckman WA, Duffie JA (1990) Diffuse fraction correlations. Sol Energy 45:1–7

Sabbagh J, Sayigh A, El-Salam E (1977) Estimation of the total solar radiation from meteorological data. Sol Energy 251(19):307–311

Said SE, Dickey D (1983) Testing for unit roots in autoregressive moving-average models with unknown order. Biometrika 71:599–607

Soares J, Oliveira AP, Božnar MZ, Mlakar P, Escobedo JF, Machado AJ (2004) Modeling hourly diffuse solar-radiation in the city of São Paulo using a neural-network technique. Appl Energy 79:201–214

Spencer JW (1982) A comparison of methods for estimating hourly diffuse solar radiation from global solar radiation. Sol Energy 29:19–32